

MIT Open Access Articles

Starting a new chapter on class Ia ribonucleotide reductases

The MIT Faculty has made this article openly available. **Please share** how this access benefits you. Your story matters.

Citation: Levitz, Talya S and Drennan, Catherine L. 2022. "Starting a new chapter on class Ia ribonucleotide reductases." *Current Opinion in Structural Biology*, 77.

As Published: 10.1016/j.sbi.2022.102489

Publisher: Elsevier BV

Persistent URL: <https://hdl.handle.net/1721.1/146796>

Version: Final published version: final published article, as it appeared in a journal, conference proceedings, or other formally published context

Terms of use: Creative Commons Attribution-NonCommercial-NoDerivs License





Starting a new chapter on class Ia ribonucleotide reductases

Talya S. Levitz¹ and Catherine L. Drennan^{1,2,3}

Abstract

Ribonucleotide reductases (RNRs) use radical-based chemistry to convert ribonucleotides into deoxyribonucleotides, an essential step in DNA biosynthesis and repair. There are multiple RNR classes, the best studied of which is the class Ia RNR that is found in *Escherichia coli*, eukaryotes including humans, and many pathogenic and nonpathogenic prokaryotes. This review covers recent advances in our understanding of class Ia RNRs, including a recent reporting of a structure of the active state of the *E. coli* enzyme and the impacts that the structure has had on spurring research into the mechanism of long-range radical transfer. Additionally, the review considers other recent structural and biochemical research on class Ia RNRs and the potential of that work for the development of anticancer and antibiotic therapeutics.



Addresses

¹ Department of Biology, Massachusetts Institute of Technology, 77 Massachusetts Avenue, Cambridge, MA 02139, USA

² Department of Chemistry, Massachusetts Institute of Technology, 77 Massachusetts Avenue, Cambridge, MA 02139, USA

³ Howard Hughes Medical Institute, Massachusetts Institute of Technology, 77 Massachusetts Avenue, Cambridge, MA 02139, USA

Corresponding author: Drennan, Catherine L, Department of Biology, Massachusetts Institute of Technology, 77 Massachusetts Avenue, Cambridge, MA 02139, USA. (cdrennan@mit.edu)

 (Levitz T.S.)
 (Drennan C.L.)

Current Opinion in Structural Biology 2022, 77:102489

This review comes from a themed issue on **Catalysis and Regulation**

Edited by **Danica Fujimori** and **Nigel Scrutton**

For a complete overview see the [Issue](#) and the [Editorial](#)

Available online xxx

<https://doi.org/10.1016/j.sbi.2022.102489>

0959-440X/© 2022 The Authors. Published by Elsevier Ltd. This is an open access article under the CC BY-NC-ND license (<http://creativecommons.org/licenses/by-nc-nd/4.0/>).

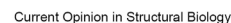
Introduction

Ribonucleotide reductase (RNR) is the only known enzyme that converts ribonucleotides into deoxyribonucleotides that are then used for cellular DNA synthesis and repair (Figure 1a). There are three main classes and many subclasses of RNRs (reviewed in Refs. [1–3]) that allow for reduction of ribonucleotides to occur in many different environmental conditions,

including anoxic environments and environments containing different metals and/or cofactors. This minireview will focus on the class Ia RNR, which is the primary aerobic RNR found in *Escherichia coli* and the only RNR found in humans.

The class Ia RNR consists of two subunits, a catalytic alpha (α) subunit and a radical-generating beta (β) subunit, which in the well-studied *E. coli* class Ia enzyme exist primarily as homodimers (α_2 and β_2) in solution [4,5] (Figure 1b). The β subunit contains a diiron cofactor that is essential for generation of a nearby stable tyrosyl radical (Y122 β in *E. coli*) [2,6–8]. During catalysis, the radical travels approximately 30 Å via a series of proton-coupled electron transfer (PCET) steps through the $\alpha_2\beta_2$ active complex to the active site where reduction of substrate occurs via a catalytic thiyl radical (Figure 1c; Reviewed in Ref. [9]). The substrate hydroxyl group is lost during catalysis with reducing equivalents coming from nearby cysteine residues that are oxidized to a disulfide (Figure 1a). A slow physical change precedes rapid radical transfer between the PCET residues, ensuring that the radical cannot get trapped at intermediate residues but allowing for no radical transfer, and thus no catalysis, to occur unless the active complex is properly assembled [10]. Tyrosine residues are uniquely suited for PCET because the thermodynamics of oxidation at physiological pH require that proton transfer accompanies electron transfer; concerted transfer prevents the formation of high-energy, charged intermediates (Reviewed in Ref. [11]).

The identity of the substrate reduced in the active site (ADP, CDP, GDP, or UDP) is allosterically regulated by the identity of the deoxyribonucleotide (dATP, dGTP, or TTP) that is bound in the nearby allosteric specificity site at the α_2 dimer interface (Figure 1b) [12–14]. Overall enzyme activity is allosterically regulated via a third nucleotide binding site at the N-terminus of α_2 and the cellular ratio of ATP to dATP (Figure 1b) [13,14]. Although all characterized class Ia RNRs are subject to allosteric activity regulation by ATP and dATP, the molecular mechanisms are not always the same. For *E. coli* class Ia RNR, dATP binding to this allosteric activity site inactivates the enzyme by shifting the equilibrium from the active $\alpha_2\beta_2$ state to the inactive $\alpha_4\beta_4$ state in which the catalytically-essential radical transfer is prevented [15–17]. For human class



In the RNR, enzyme inhibition by dATP appears to be accompanied by formation of a stable $\alpha 6$ state that prevents $\alpha 2$ and $\beta 2$ from interacting in a catalytically competent fashion for radical transfer [18–21].

Although the class Ia RNR has been purified and studied for almost six decades, recent advances in structural determination and spectroscopy have enhanced our understanding of the mechanism of catalysis of this

essential enzyme. In particular, cryo-electron microscopy (cryo-EM) developments have enabled the structure of the elusive active $\alpha_2\beta_2$ complex to be solved [22,23]. This review will cover how the $\alpha_2\beta_2$ structure visualized many new components of the enzyme complex and generated numerous hypotheses regarding the mechanisms of radical transfer and enzyme turnover. The elucidation of the $\alpha_2\beta_2$ structure identified residues and interactions that can and have been probed using various types of spectroscopy, including electron paramagnetic resonance (EPR), electron nuclear double resonance (ENDOR), and Fourier-transform infrared (FTIR) spectroscopies [24–29]. Lastly, recent structures of other class Ia enzymes from different organisms allow for a comparison to the canonical *E. coli* structure and offer promising anticancer and antimicrobial targets [19,30–32].

Solving the $\alpha_2\beta_2$ structure

Solution-state methods determined the active state of the *E. coli* RNR to be $\alpha_2\beta_2$ early on, and this determination was confirmed by more advanced methods as the field of biochemistry progressed [4,5,15]. However, despite modeling of how the two subunits fit together and the solving of many structures of the individual subunits, until recently there was no structure of the $\alpha_2\beta_2$ complex [7,14,33]. In contrast, the *E. coli* class Ia RNR inactive state was found to be $\alpha_4\beta_4$ using multiple solution-state methods [15,16] and was solved by crystallography in 2012 with further substrate/effector pairs in 2016 [12,17], and human and yeast α_6 complexes were also solved by cryo-EM and crystallography during this period [19,20]. However, the $\alpha_2\beta_2$ complex remained elusive due to the transitory nature of the complex (k_{off} of β_2 from α_2 is approximately $60\text{--}75\text{ s}^{-1}$ [34]) being incompatible with crystal formation and difficult to capture on EM grids. A recent explosion of hardware and software developments in the field of cryo-EM [35,36], along with key residue substitutions, enabled the determination of the $\alpha_2\beta_2$ structure of the *E. coli* RNR (Figure 2a) [22]. Substitution of the unnatural amino acid trifluorotyrosine for the radical-harboring tyrosine (Y122 β) as well as another mutation (E52Q β) along the α/β interface allowed for persistence of the $\alpha_2\beta_2$ complex for long enough that it could be captured via cryo-EM (Figure 2a) [22,23]. Glutamate 52 was first identified as a residue of interest because of its fully conserved status among 80 class Ia RNRs; the combination of substitutions for cryo-EM was determined empirically through efforts of the Nocera and Stubbe labs over more than a decade [7,23,37]. The structure of the *E. coli* class Ia RNR that was elucidated through these efforts has relevance to other class Ia RNRs, which, in contrast to their diverse inactive states, are postulated to form a similar $\alpha_2\beta_2$ active complex, allowing for use of the *E. coli* structure to formulate new

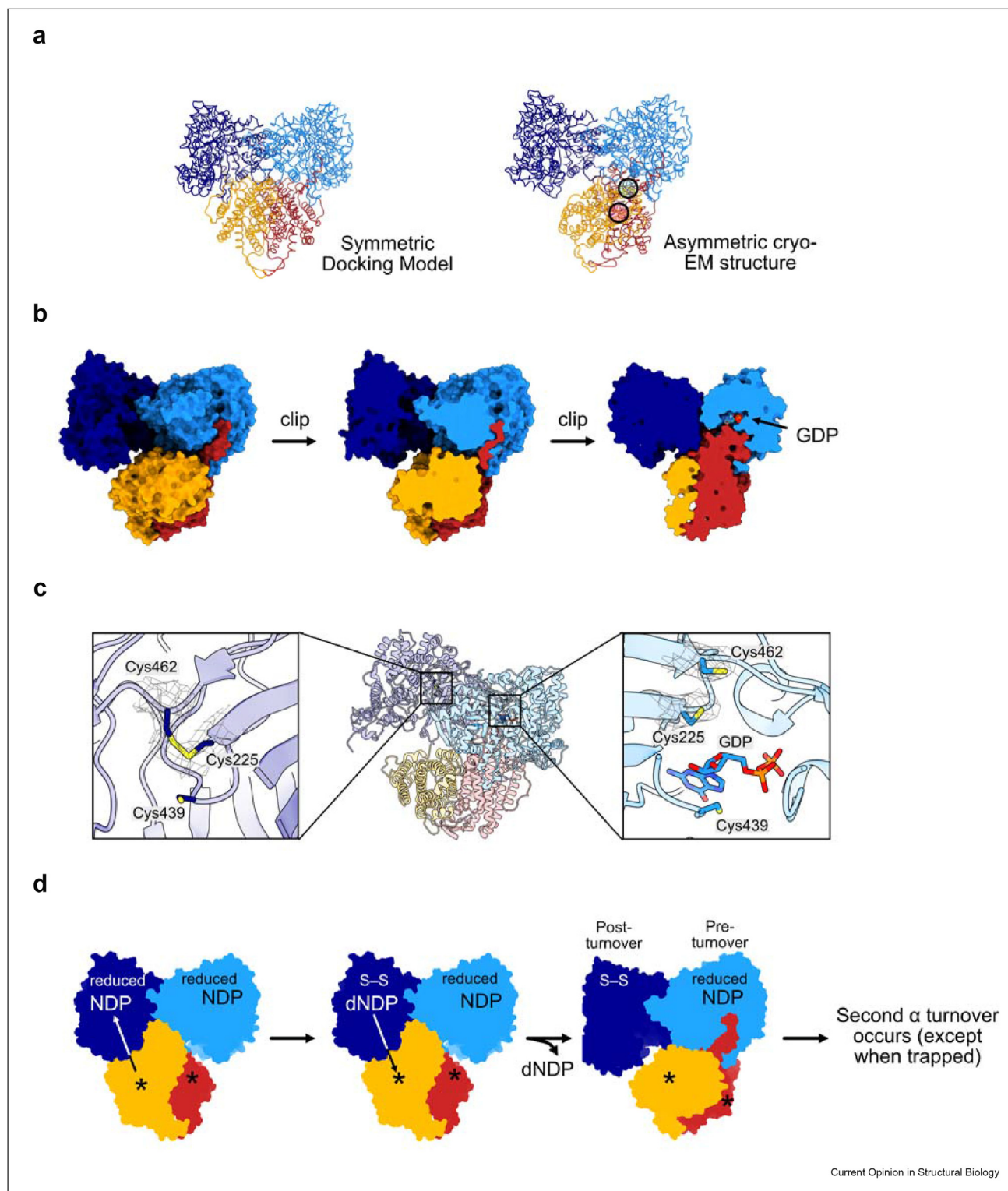
hypotheses regarding similarities and differences between other class Ia active states [1,2].

The $\alpha_2\beta_2$ structure of *E. coli* Ia RNR provided considerable insight into the molecular mechanisms of RNR catalysis. First, the structure is strikingly asymmetric, unlike the previous docking model which was symmetric [33]: the α_2/β_2 interface is primarily formed between one α monomer and β_2 [15,22,33] (Figure 2a). β_2 presumably has to swing from one α subunit to the other for catalysis to occur in both α subunits, indicating that only one α/β radical transfer pathway can be generated at a time, consistent with observations of half-of-sites reactivity [23,38,39]. Second, the elusive β tail (residues 341–375) that contains the essential PCET residue Y356 was finally visualized [22] (Figure 2b). The β tail was disordered in all previous β -only and $\alpha_4\beta_4$ structures (see Ref. [40] for a review of many of the determined structures, all of which have disordered β tails; more recent structures containing similarly disordered tails include [12,41]). The structure showed that in the $\alpha_2\beta_2$ active state, the β tail extends up from β into the active site in α , coming in van der Waals contact with bound substrate, turns and extends down again, occluding access to the active site [15,22,33] (Figure 2b). This proximity of the β tail to the active site elucidated that β departure, and thus disassembly of the PCET pathway, is necessary in order for product dissociation to occur. Additionally, the binding site for the β tail is made up of the substrate itself and of residues that move when substrate binds, indicating that substrate binding may facilitate PCET pathway assembly [22]. Third, the structure showed that the active site cysteines of the two α monomers were in different oxidation states: whereas the α subunit in contact with β_2 was in a preturnover state (cysteines reduced), the α subunit not in contact with β_2 appeared to be in a postturnover (cysteines oxidized to a disulfide) state [22] (Figure 2c). A comparison of preturnover and postturnover states shows shrinkage of the active site upon disulfide formation [14], providing a possible molecular mechanism for β tail “release” and β_2 “swinging” between active sites on α_2 : disulfide formation could “push” on the product deoxyribonucleotide, which in turn would put pressure on β to release following back-radical transfer (Figure 2d) [22].

Structure-guided investigations into the PCET pathway

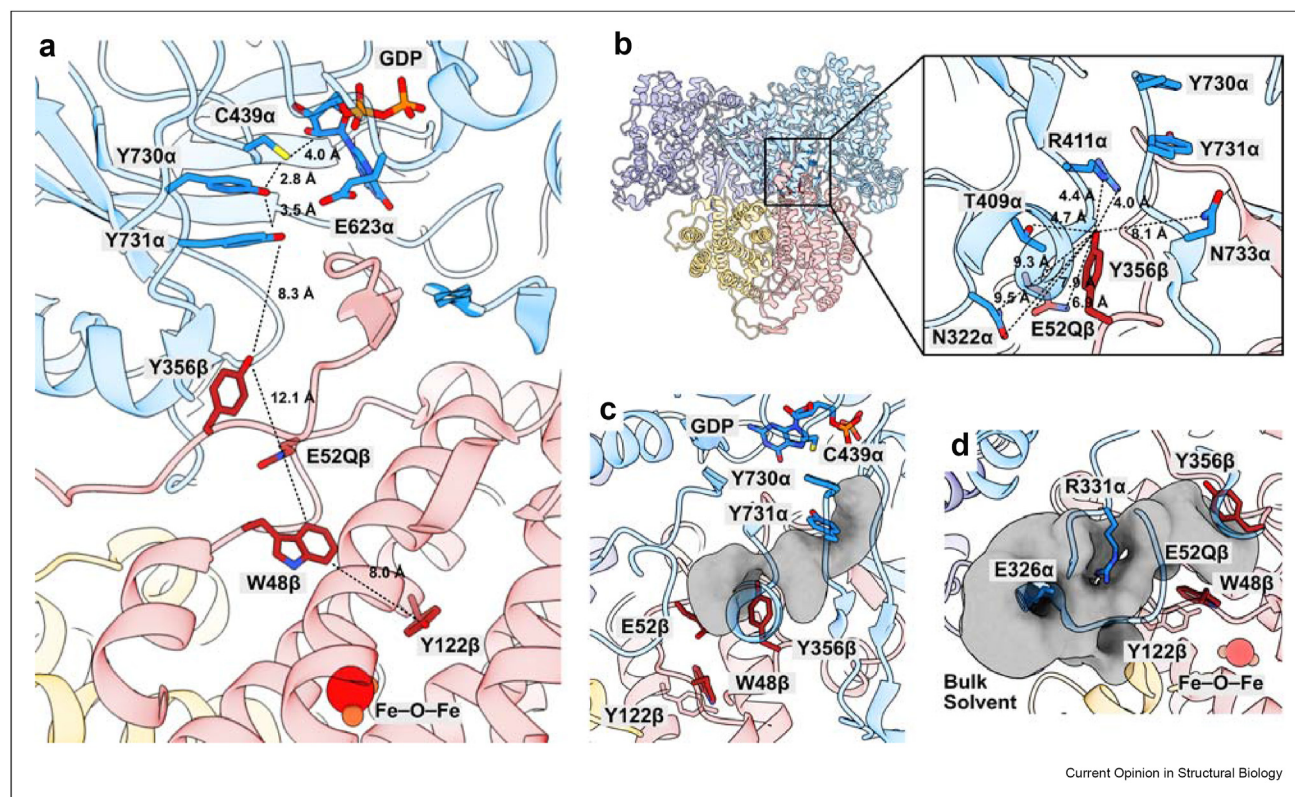
All the residues in the PCET pathway are fully resolved in the $\alpha_2\beta_2$ structure [7,9,33]. Visualization of the residues provided insight into the local environment of PCET residues, the potential players in proton transfer to/from PCET residues, and the electron transfer distances traveled between PCET residues [15,22,33] (Figure 3a). The structure confirmed that the residue-to-

Figure 2



The *E. coli* class Ia RNR $\alpha_2\beta_2$ cryo-EM structure provided molecular evidence for sequential radical firing within the dimer, mechanisms of substrate release, and preparation for the next cycle of catalysis. (a) A comparison of the symmetric $\alpha_2\beta_2$ docking model that was created based on aligning the two-fold axes of the α_2 and β_2 subunit structures (left) and the asymmetric $\alpha_2\beta_2$ cryo-EM structure (right) of the *E. coli* class Ia RNR. Alpha subunits are shown in navy and light blue whereas beta subunits are shown in red and orange. The structure was solved using two substitutions in the beta subunit, Y122F₃Y (circled on one subunit in magenta) and E52Q (circled on one subunit in cyan). (b) One beta subunit (red) contacting the alpha subunit (light blue) has tail residues that extend into the active site, blocking release of the GDP substrate (spheres colored cyan and by heteroatom;

Figure 3



residue distances within the α subunit (2.8–3.5 Å) are shorter than in the β subunit (8.0–12.1 Å), consistent with the idea that collinear transfer, where the proton and electron move between the same donor and acceptor groups, occurs in the α subunit, whereas orthogonal electron and proton transfer, where the proton and electron come from the same group but end up on different molecules, occurs in the β subunit [9,22] (see Figure 1c for proposed PCET pathway). Of note, the position of W48 β approximately midway between PCET

residues Y122 β and Y356 β has renewed interest in whether this residue plays a direct role in the radical transfer between subunits. W48 β is essential for radical cofactor biogenesis, but its involvement in radical transfer has not been conclusively demonstrated [2,42–44].

Overall, the $\alpha_2\beta_2$ structure generated new hypotheses that could be tested using both biochemical and computational techniques. Many of these recent studies focused on residues identified as being along the PCET

indicated by arrow). The structure is shown on three different clipping planes from left to right. (c) The two different active sites in the $\alpha_2\beta_2$ structure contain different oxidation states of cysteine residues C225 and C462 as well as a presence or absence of substrate (GDP). The catalytic cysteine C439 is also shown as sticks. Note that the oxidized active site (left) is shrunk compared to the reduced active site (right). (d) A model for catalysis in the asymmetric $\alpha_2\beta_2$ complex. An $\alpha_2\beta_2$ complex fully loaded with substrate and containing two reduced active site cysteine residue pairs (left) would undergo PCET from β to the α subunit, reduction of substrate, and oxidation of active site cysteine residues. The radical then returns to the same β subunit (middle), product leaves the α subunit, and the β_2 swings over to the other α subunit, creating one post-turnover α and one pre-turnover α (left). A second round of turnover would then occur in the absence of a substitution that traps the complex in this state. All images generated using PDB 6W4X (except for docking model from Ref. [33]) and ChimeraX [22,58].

pathway and on the potential role in proton transfer to water molecules, which were not visualized in the cryo-EM structure due to the structure's resolution (Figure 1c). One study, a molecular dynamics study, conducted on the $\alpha 2\beta 2$ structure indicated that movement of Y731 α is likely critical for PCET to occur, alternatively allowing for a shorter distance than 8.3 Å between Y356 β and Y731 α by Y731 α flipping down (see Figure 3a) and then restoring the close 3.5 Å distance between Y731 α and Y730 α by Y731 α flipping back up [24]. This finding corroborates previous work using pulsed electron–electron double resonance (PELDOR) spectroscopy demonstrating the flexibility of Y731 α [45]. Additionally, α/β interfacial water molecules, long-thought to be important in the PCET pathway, were identified in silico as the primary proton acceptors from Y356 β and Y731 α (Figure 3a) [24,46]. Closer inspection of the environment surrounding Y356 β indicates a lack of a close (less than 3.5 Å) polar residue to serve as a direct proton donor/acceptor (Figure 3b). Instead, distances suggest that nearby polar residues could play an indirect role in the acid/base chemistry via water molecules. The structure shows that there is ample room for water molecules surrounding both Y356 β and Y731 α (Figure 3b and c). A further computational study by Reinhardt and colleagues on the $\alpha 2\beta 2$ structure using quantum mechanical and molecular mechanical free energy simulations of PCET between residues Y730 α and Y731 α indicate that when the protein is in the pre-turnover state, forward radical transfer (Y731 α > Y730 α) is thermodynamically favored, whereas backward radical transfer is favored in the post-turnover state [25]. The role of a glutamate residue E623 α was also identified as a residue of interest for future study (Figure 3a). Experimental validation of the hypotheses generated by the molecular modeling studies are eagerly awaited.

One such experimental study focused on Y356 β and its interactions with E52 β (Figure 3a and b) [26]. The study by Cui et al. found using transient absorbance spectroscopy followed by flash quenching that E52 β is part of a water channel at the α/β subunit interface that facilitates rapid proton transfer to the bulk solvent (Figure 3d); substitution of E52 β to Q generates a variant that is unable to complete Y356 oxidation, likely due to the inability to deprotonate the hydroxyl group of the Y356 β side chain (Y–OH) to generate a tyrosyl radical (Y–O•) [26]. This experiment also helped to explain why the E52Q substitution stalled radical transfer, thus preserving the $\alpha 2\beta 2$ state for structural analysis [22]. Another recent study looking at the role of Y356 β using reaction-induced FTIR spectroscopy found that restructuring of Y356 β occurs upon formation of the $\alpha 2\beta 2$ complex, consistent with its visualization within the $\alpha 2\beta 2$ structure but not previous structures and indicating that formation of the catalytic complex requires movement of PCET residues into a state competent for radical transfer [27]. At the other end of

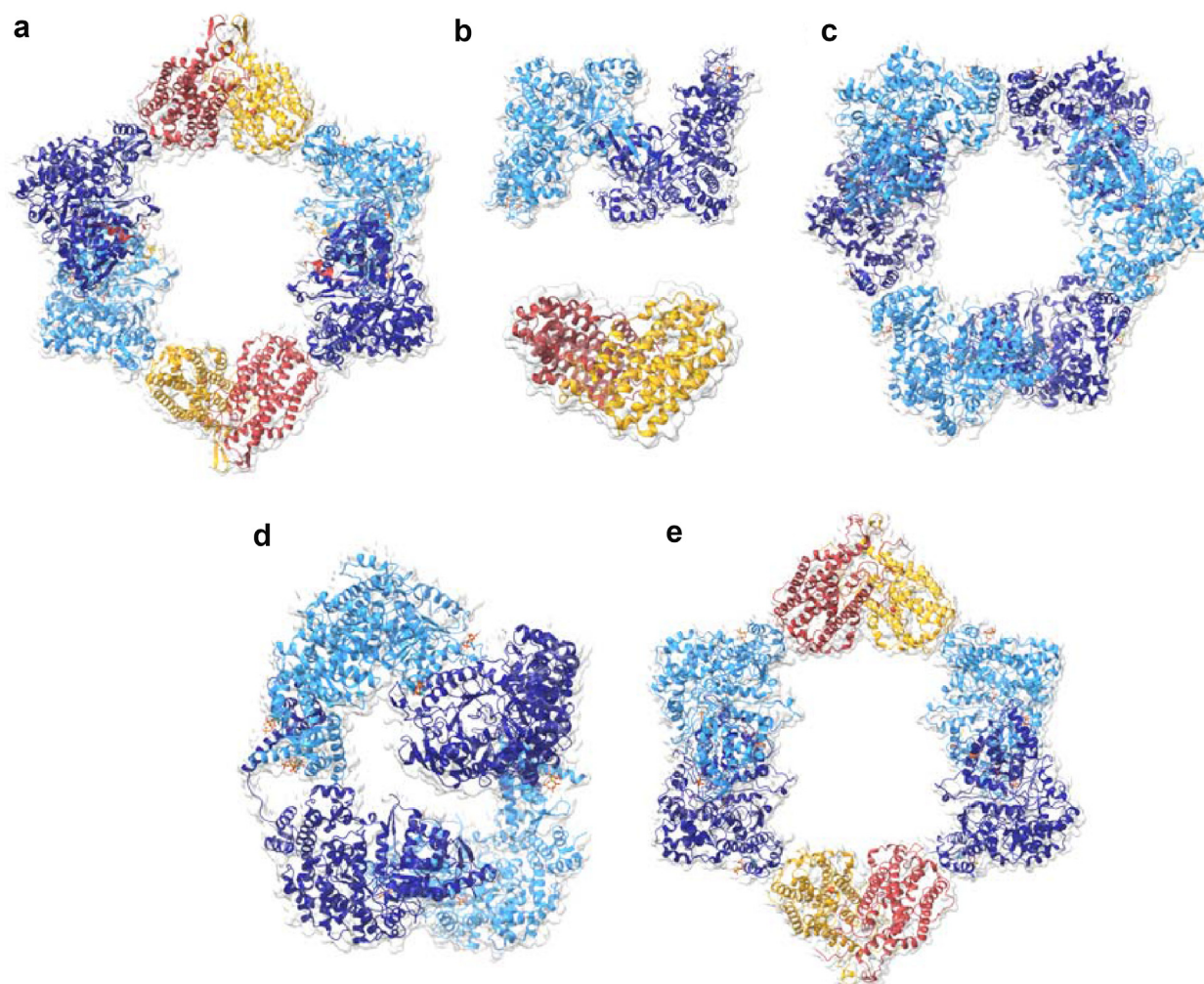
the radical transfer pathway in β , a separate study used both EPR and ENDOR to characterize the Y122 β radical in whole cells and in vitro and determined that the structure and electrostatic environment of Y122 β are identical under in vivo and in vitro conditions; this finding provides physiological relevance to previous in vitro studies on the Y122 β species [29].

The role of water molecules along the entire PCET pathway was additionally probed using ^{17}O high-frequency ENDOR [28]. ENDOR and PELDOR spectroscopy have been utilized in past studies of RNR to determine residue-to-residue distances along the PCET pathway; these techniques are how the PCET distance was estimated to be 35–40 Å [47] before the $\alpha 2\beta 2$ structure measured it as 32 Å. In the aforementioned study, Hecker and colleagues established the presence of ordered water molecules at three positions along the PCET pathway: Y356 β , Y731 α , and Y730 α (Figure 3a,c). In these experiments, three RNR variants were generated to trap a radical species at each of the three Y positions, with variants subjected to spectroscopic methods to identify interactions between the Y radical species and the ^{17}O of a water molecule [28]. The water to Y distance was in the 2.8–3.1 Å range in all cases [28]. Although the necessity of water molecules in the process of RNR PCET has been postulated for decades [48], recent advances are beginning to provide molecular explanations for the role of water molecules and polar residues along this atypically-long and complex PCET pathway.

Looking forward: applications of knowledge of RNR structure and mechanism

The *E. coli* RNR enzyme has been the workhorse for investigations of class Ia RNRs since its discovery, and although it is valuable to have one system that is thoroughly understood, it is also important to recognize and comment on the work that is being done on other class Ia RNR enzymes that is revealing both similarities and differences to the *E. coli* enzyme. For example, structural analyses of the class Ia RNR from the hyperthermophile *Aquifex aeolicus* identified a unique intein region in the *A. aeolicus* RNR beta subunit that is important for iron incorporation. The authors also found two ATP molecules bound in the N-terminal cone domain (Figure 4b) [30]. The study additionally probed the active and inactive oligomeric states of the *A. aeolicus* RNR using solution-state methods and found that the enzyme forms an $\alpha 2\beta 2$ active state and likely forms an $\alpha 4\beta 4$ inactive state [30]. In another study, interactions of the components of the pseudorabies virus class Ia RNR, which has two large and two small subunits, have been recently mapped using co-immunoprecipitation and colocalization analyses [49]. The human $\alpha 6$ inactive state, which contrasts the *E. coli* $\alpha 4\beta 4$ inactive state (Figure 4a), has also been elucidated by cryo-EM to 3.3 Å resolution [19] (Figure 4c), and the *Pseudomonas*

Figure 4



Current Opinion in Structural Biology

Diversity of recent solved structures of class Ia RNRs as compared to the *E. coli* class Ia RNR. For all structures, α monomers are shown as navy and blue, whereas β monomers are shown as red and orange. (a) Structure of the *E. coli* class Ia RNR in the $\alpha_4\beta_4$ inhibited state. Figure generated from PDB 5CNS [12]. (b) Structures of *Aquifex aeolicus* α_2 (top) and β_2 (bottom) complexes. Figures generated from PDB 7AGJ [30]. (c) The α_6 structure of the dATP-inhibited human RNR enzyme. Figure generated from PDB 6AUI [19]. (d) The α_4 structure of the dATP-inhibited *Pseudomonas aeruginosa* RNR. Figure generated from PDB 5IM3 [32]. (e) The $\alpha_4\beta_4$ structure of the dATP-inhibited *Neisseria gonorrhoeae* RNR. Figure generated from PDB 7MDI [31]. All images generated using UCSF ChimeraX [58].

aeruginosa α_4 inactive state has been solved crystallographically with 2 dATP molecules present in each cone domain [32] (Figure 4d). The diversity of structures of class Ia RNRs opens the door for species-specific structure-based drug design of both cancer drugs and antibiotics (see Refs. [2,50] for review; FDA-approved anticancer drugs, but not antibiotics, are currently in use that specifically target RNR). Recently, a cryo-EM structure of the class Ia RNR from *Neisseria gonorrhoeae* was published alongside a paper identifying new compounds that target the *N. gonorrhoeae* RNR, highlighting

the promise that RNR has as a new antibiotic target in a time where new targets are sorely needed [31,51–53] (Figure 4e). Computational studies have also recently been completed investigating inhibitors of the *Chlamydia felis* and *Elizabethkingia spp.* class Ia RNRs [54,55], as well as probing both established and novel anticancer compounds [56,57], indicating RNR's current utility and future promise as a drug target as well as the necessity for more structural knowledge regarding both the human class Ia RNR and class Ia RNRs from emerging and established pathogens.

Conclusions

The elucidation of a structure of an active $\alpha\beta\beta_2$ state is not the end of the story of this enigmatic RNR enzyme family, but rather the beginning of a new chapter. Already biochemical and computational studies have begun to probe residues highlighted by the structural data, providing new insight into long-range PCET and into the conformational gymnastics that this enzyme appears to employ. Further structural studies on the $\alpha\beta\beta_2$ complex will likely lead to improved resolution and the visualization of water molecules that line the PCET pathway. Additionally, structural and biochemical studies on other class Ia RNRs, including those from human and pathogenic RNRs, will be instrumental in understanding the mechanism of current RNR inhibitors as well as in formulation and study of the next generation of RNR inhibitors.

Funding

This work was supported by NIH grant GM126982 to C.L.D. and NSF GRFP 2017246757 to T.S.L. as well as NIH T32 Training Grant 5T32GM007287 awarded to the MIT Biology Department. C.L.D. is a Howard Hughes Medical Institute Investigator and Senior Fellow for the Canadian Institute for Advanced Research Bio-Inspired Solar Energy program.

Conflict of interest statement

Nothing declared.

Data availability

No data was used for the research described in the article.

References

Papers of particular interest, published within the period of review, have been highlighted as:

* of special interest

** of outstanding interest

- Torrents E: **Ribonucleotide reductases: essential enzymes for bacterial life**. *Front Cell Infect Microbiol* 2014, **4**.
- Greene BL, Kang G, Cui C, Bennati M, Nocera DG, Drennan CL, Stubbe J: **Ribonucleotide reductases: structure, chemistry, and metabolism suggest new therapeutic targets**. *Annu Rev Biochem* 2020, **89**:45–75.
- Ruskoski TB, Boal AK: **The periodic table of ribonucleotide reductases**. *J Biol Chem* 2021, **294**:101137, <https://doi.org/10.1016/j.jbc.2021.101137>.
- Brown NC, Canellakis ZN, Lundin B, Reichard P, Thelander L: **Ribonucleoside diphosphate reductase. Purification of the two subunits, proteins B1 and B2**. *Eur J Biochem* 1969, **9**: 561–573.
- Thelander L: **Physicochemical characterization of ribonucleoside diphosphate reductase from Escherichia coli**. *J Biol Chem* 1973, **248**:4591–4601.
- Atkin CL, Thelander L, Reichard P, Lang G: **Iron and free radical in ribonucleotide reductase. Exchange of iron and Mössbauer spectroscopy of the protein B2 subunit of the Escherichia coli enzyme**. *J Biol Chem* 1973, **248**:7464–7472.
- Nordlund P, Sjöberg B-M, Eklund H: **Three-dimensional structure of the free radical protein of ribonucleotide reductase**. *Nature* 1990, **345**:593–598.
- Zhang C, Liu G, Huang M: **Ribonucleotide reductase metal-locofactor: assembly, maintenance and inhibition**. *Front Biol* 2014, **9**:104–113.
- Reece SY, Seyedsayamdost MR: **Long-range proton-coupled electron transfer in the Escherichia coli class Ia ribonucleotide reductase**. *Essays Biochem* 2017, **61**:281–292.
- Ge J, Yu G, Ator MA, Stubbe J: **Pre-steady-state and steady-state kinetic analysis of E. coli class I ribonucleotide reductase**. *Biochemistry* 2003, **42**:10071–10083.
- Reece SY, Nocera DG: **Proton-coupled electron transfer in biology: results from synergistic studies in natural and model systems**. *Annu Rev Biochem* 2009, **78**:673–699.
- Zimanyi CM, Chen PY-T, Kang G, Funk MA, Drennan CL: **Molecular basis for allosteric specificity regulation in class Ia ribonucleotide reductase from Escherichia coli**. *Elife* 2016, **5**, e07141.
- Brown NC, Reichard P: **Role of effector binding in allosteric control of ribonucleoside diphosphate reductase**. *J Mol Biol* 1969, **46**:39–55.
- Eriksson M, Uhlin U, Ramaswamy S, Ekberg M, Regnström K, Sjöberg B-M, Eklund H: **Binding of allosteric effectors to ribonucleotide reductase protein R1: reduction of active-site cysteines promotes substrate binding**. *Structure* 1997, **5**: 1077–1092.
- Ando N, Brignole EJ, Zimanyi CM, Funk MA, Yokoyama K, Asturias FJ, Stubbe J, Drennan CL: **Structural interconversions modulate activity of Escherichia coli ribonucleotide reductase**. *Proc Natl Acad Sci USA* 2011, **108**:21046–21051.
- Rofougaran R, Crona M, Vodnala M, Sjöberg B-M, Hofer A: **Oligomerization status directs overall activity regulation of the Escherichia coli class Ia ribonucleotide reductase**. *J Biol Chem* 2008, **283**:35310–35318.
- Zimanyi CM, Ando N, Brignole EJ, Asturias FJ, Stubbe J, Drennan CL: **Tangled up in knots: structures of inactivated forms of E. coli class Ia ribonucleotide reductase**. *Structure* 2012, **20**:1374–1383.
- Ando N, Li H, Brignole EJ, Thompson S, McLaughlin MI, Page JE, Asturias FJ, Stubbe J, Drennan CL: **Allosteric inhibition of human ribonucleotide reductase by dATP entails the stabilization of a hexamer**. *Biochemistry* 2016, **55**:373–381.
- Brignole EJ, Tsai K-L, Chittuluru J, Li H, Aye Y, Penczek PA, Stubbe J, Drennan CL, Asturias F: **3.3-Å resolution cryo-EM structure of human ribonucleotide reductase with substrate and allosteric regulators bound**. *Elife* 2018, **7**.
- Fairman JW, Wijerathna SR, Ahmad MF, Xu H, Nakano R, Jha S, Prendergast J, Welin RM, Flodin S, Roos A, et al.: **Structural basis for allosteric regulation of human ribonucleotide reductase by nucleotide-induced oligomerization**. *Nat Struct Mol Biol* 2011, **18**:316–322.
- Rofougaran R, Vodnala M, Hofer A: **Enzymatically active mammalian ribonucleotide reductase exists primarily as an alpha6beta2 octamer**. *J Biol Chem* 2006, **281**: 27705–27711.
- Kang G, Taguchi AT, Stubbe J, Drennan CL: **Structure of a trapped radical transfer pathway within a ribonucleotide reductase holoenzyme**. *Science* 2020, **368**:424–427.
- A presentation of the $\alpha\beta\beta_2$ E. coli RNR structure solved by cryo-EM. This is the first structure of an active state RNR.
- Lin Q, Parker MJ, Taguchi AT, Ravichandran K, Kim A, Kang G, Shao J, Drennan CL, Stubbe J: **Glutamate 52-β at the α/β subunit interface of Escherichia coli class Ia ribonucleotide reductase is essential for conformational gating of radical transfer**. *J Biol Chem* 2017, **292**:9229–9239.
- Reinhardt CR, Li P, Kang G, Stubbe J, Drennan CL, Hammes-Schiffer S: **Conformational motions and water networks at the α/β interface in E. coli ribonucleotide reductase**. *J Am Chem Soc* 2020, **142**:13768–13778.

Performs MD simulations on the new $\alpha 2\beta 2$ structure to examine the structure and fluctuations of interfacial waters and interfacial residues along the PCET pathway. Allows for visualization of the conformational sampling space of different residues as well as important hydrogen bonds between residues and interfacial water molecules.

25. Reinhardt CR, Sayfutyarova ER, Zhong J, Hammes-Schiffer S: **Glutamate mediates proton-coupled electron transfer between tyrosines 730 and 731 in *Escherichia coli* ribonucleotide reductase.** *J Am Chem Soc* 2021, **143**:6054–6059.

Performs quantum mechanical and molecular mechanical free energy simulations of PCET between tyrosine residues Y730 and Y731 on the $\alpha 2\beta 2$ structure, showing forward radical transfer between residues is thermodynamically favored in the pre-turnover state and backward radical transfer is favored in the post-turnover state. Also elucidated the role of E623 in facilitating forward radical transfer between Y730 and Y731, reinforcing the role of PCET-adjacent residues in facilitating radical transfer.

26. Cui C, Greene BL, Kang G, Drennan CL, Stubbe J, Nocera DG: **Gated proton release during radical transfer at the subunit interface of ribonucleotide reductase.** *J Am Chem Soc* 2021, **143**:176–183.

Shows experimentally that the oxidation of Y356 β is regulated by proton release involving E52 β , which is part of a water channel at the subunit interface for rapid proton transfer to the bulk solvent. Reinforces the role of non-PCET residues in facilitating PCET and elucidates why the E52Q mutation enabled persistence of the *E. coli* $\alpha 2\beta 2$ complex.

27. Watson RA, Offenbacher AR, Barry BA: **Detection of catalytically linked conformational changes in wild-type class Ia ribonucleotide reductase using reaction-induced FTIR spectroscopy.** *J Phys Chem B* 2021, **125**:8362–8372.

Presents a reaction-induced Fourier transform infrared (RIFTIR) spectroscopic method to monitor the mechanism of the active, wild-type RNR $\alpha 2\beta 2$ complex. This method is used to experimentally and noninvasively probe conformational and secondary structural changes that occur during catalysis.

28. Hecker F, Stubbe J, Bennati M: **Detection of water molecules on the radical transfer pathway of ribonucleotide reductase by ^{17}O electron-nuclear double resonance spectroscopy.** *J Am Chem Soc* 2021, **143**:7237–7241.

Uses ^{17}O high-frequency electron-nuclear double resonance (ENDOR) in conjunction with H_2^{17}O -labeled protein buffer to establish the presence of ordered water molecules within the $\alpha 2\beta 2$ *E. coli* RNR active state. This allows for more granular models of water coupling along the PCET pathway in the active state of the enzyme.

29. Meichsner SL, Kutin Y, Kusanmascheff M: **In-cell characterization of the stable tyrosyl radical in *E. coli* ribonucleotide reductase using advanced EPR spectroscopy.** *Angew Chem Int Ed Engl* 2021, **60**:19155–19161.

30. Rehling D, Scaletti ER, Rozman Grinberg I, Lundin D, Sahlin M, Hofer A, Sjöberg B-M, Stenmark P: **Structural and biochemical investigation of class I ribonucleotide reductase from the hyperthermophile *Aquifex aeolicus*.** *Biochemistry* 2022, **61**:92–106.

Presents structures of the *Aquifex aeolicus* RNR α and β subunits and identifies and probes an inter region that facilitates metal incorporation into the β subunit. Illustrates the diversity of sequence space and assembly within the class Ia RNRs.

31. Levitz TS, Brignole EJ, Fong I, Darrow MC, Drennan CL: **Effects of chameleon dispense-to-plunge speed on particle concentration, complex formation, and final resolution: a case study using the *Neisseria gonorrhoeae* ribonucleotide reductase inactive complex.** *J Struct Biol* 2022, **214**, 107825.

Presents a structure of the *Neisseria gonorrhoeae* RNR, which is a promising novel antibiotic target.

32. Jonna VR, Crona M, Rofougaran R, Lundin D, Johansson S, Brännström K, Sjöberg B-M, Hofer A: **Diversity in overall activity regulation of ribonucleotide reductase.** *J Biol Chem* 2015, **290**:17339–17348.

33. Uhlin U, Eklund H: **Structure of ribonucleotide reductase protein R1.** *Nature* 1994, **370**:533.

34. Minnihan EC, Ando N, Brignole EJ, Olshansky L, Chittuluru J, Asturias FJ, Drennan CL, Nocera DG, Stubbe J: **Generation of a stable, aminotyrosyl radical-induced $\alpha 2\beta 2$ complex of *Escherichia coli* class Ia ribonucleotide reductase.** *Proc Natl Acad Sci USA* 2013, **110**:3835–3840.

35. Nogales E: **The development of cryo-EM into a mainstream structural biology technique.** *Nat Methods* 2016, **13**:24–27.

36. Cheng Y: **Single particle cryo-EM – how did it get here and where will it go.** *Science* 2018, **361**:876–880.

37. Lundin D, Torrents E, Poole AM, Sjöberg B-M: **RNRdb, a curated database of the universal enzyme family ribonucleotide reductase, reveals a high level of misannotation in sequences deposited to Genbank.** *BMC Genom* 2009, **10**:589.

38. Salowe SP, Ator MA, Stubbe J: **Products of the inactivation of ribonucleoside diphosphate reductase from *Escherichia coli* with 2'-azido-2'-deoxyuridine 5'-diphosphate.** *Biochemistry* 1987, **26**:3408–3416.

39. Salowe S, Bollinger JM, Ator M, Stubbe J, McCracken J, Peisach J, Samano MC, Robins MJ: **Alternative model for mechanism-based inhibition of *Escherichia coli* ribonucleotide reductase by 2'-azido-2'-deoxyuridine 5'-diphosphate.** *Biochemistry* 1993, **32**:12749–12760.

40. Eklund H, Uhlin U, Färnegårdh M, Logan DT, Nordlund P: **Structure and function of the radical enzyme ribonucleotide reductase.** *Prog Biophys Mol Biol* 2001, **77**:177–268.

41. Oyala PH, Ravichandran KR, Funk MA, Stucky PA, Stich TA, Drennan CL, Britt RD, Stubbe J: **Biophysical characterization of fluorotyrosine probes site-specifically incorporated into enzymes: *E. coli* ribonucleotide reductase as an example.** *J Am Chem Soc* 2016, **138**:7951–7964.

42. Krebs C, Chen S, Baldwin J, Ley BA, Patel U, Edmondson DE, Huynh BH, Bollinger JM: **Mechanism of rapid electron transfer during oxygen activation in the R2 subunit of *Escherichia coli* ribonucleotide reductase. 2. Evidence for and consequences of blocked electron transfer in the W48F variant.** *J Am Chem Soc* 2000, **122**:12207–12219.

43. Saleh L, Kelch BA, Pathickal BA, Baldwin J, Ley BA, Bollinger JM: **Mediation by indole analogues of electron transfer during oxygen activation in variants of *Escherichia coli* ribonucleotide reductase R2 lacking the electron-shuttling tryptophan 48.** *Biochemistry* 2004, **43**:5943–5952.

44. Pagba CV, McCaslin TG, Veglia G, Porcelli F, Yohannan J, Guo Z, McDaniel M, Barry BA: **A tyrosine-tryptophan dyad and radical-based charge transfer in a ribonucleotide reductase-inspired maquette.** *Nat Commun* 2015, **6**, 10010.

45. Kusanmascheff M, Lee W, Nick TU, Stubbe J, Bennati M: **Radical transfer in *E. coli* ribonucleotide reductase: a NH2Y731/R411A- α mutant unmasks a new conformation of the pathway residue 731.** *Chem Sci* 2016, **7**:2170–2178.

46. Nick TU, Ravichandran KR, Stubbe J, Kusanmascheff M, Bennati M: **Spectroscopic evidence for a H bond network at Y356 located at the subunit interface of active *E. coli* ribonucleotide reductase.** *Biochemistry* 2017, **56**:3647–3656.

47. Seyedsayamdost MR, Chan CTY, Mugnaini V, Stubbe J, Bennati M: **PELDOR spectroscopy with DOPA- $\beta 2$ and NH2Y- $\alpha 2s$: distance measurements between residues involved in the radical propagation pathway of *E. coli* ribonucleotide reductase.** *J Am Chem Soc* 2007, **129**:15748–15749.

48. Minnihan EC, Nocera DG, Stubbe J: **Reversible, long-range radical transfer in *E. coli* class Ia ribonucleotide reductase.** *Acc Chem Res* 2013, **46**:2524–2535.

49. Lyu C, Li W-D, Peng J-M, Cai X-H: **Identification of interaction domains in the pseudorabies virus ribonucleotide reductase large and small subunits.** *Vet Microbiol* 2020, **246**, 108740.

50. Shao J, Liu X, Zhu L, Yen Y: **Targeting ribonucleotide reductase for cancer therapy.** *Expert Opin Ther Targets* 2013, **17**:1423–1437.

51. Narasimhan J, Letinski S, Jung SP, Gerasuto A, Wang J, Arnold M, Chen G, Hedrick J, Dumble M, Ravichandran K, et al.: **Ribonucleotide reductase, a novel drug target for gonorrhea.** *Elife* 2022, **11**, e67447.

A biological and structural study of new compounds that target the *Neisseria gonorrhoeae* RNR. Presents two new compounds that specifically inhibit the gonorrheal RNR and demonstrates their in vivo and in vitro activities as well as negative stain structural data showing the *N. gonorrhoeae* RNR forms an $\alpha 4\beta 4$ complex similar to the *E. coli*

RNR. The first presentation of drugs that specifically target a microbial RNR.

52. Murray CJ, Ikuta KS, Sharara F, Swetschinski L, Aguilar GR, Gray A, Han C, Bisignano C, Rao P, Wool E, *et al.*: **Global burden of bacterial antimicrobial resistance in 2019: a systematic analysis.** *Lancet* 2022, **399**:629–655.
53. Zaman SB, Hussain MA, Nye R, Mehta V, Mamun KT, Hossain N: **A review on antibiotic resistance: alarm bells are ringing.** *Cureus* 2017, **9**:e1403.
54. Ravindranath BS, Vishnu Vinayak S, Chandra Mohan V: **RNR inhibitor binding studies of *Chlamydia felis*: insights from in silico molecular modeling, docking, and simulation studies.** *J Biomol Struct Dyn* 2021, <https://doi.org/10.1080/07391102.2021.1930160>.
55. Mahfuz AMUB, Iqbal MN, Opazo FS, Zubair-Bin-Mahfuj AM: **Characterization of ribonucleotide reductases of emerging pathogens *Elizabethkingia anophelis* and *Elizabethkingia meningoseptica* and streptonigrin as their inhibitor: a computational study.** *J Biomol Struct Dyn* 2021, <https://doi.org/10.1080/07391102.2021.1930166>.
56. Channar PA, Aziz M, Ejaz SA, Chaudhry G-E-S, Saeed A, Ujan R, Hasan A, Ejaz SR, Saeed A: **Structural and functional insight into thiazolidinone derivatives as novel candidates for anti-cancer drug design: in vitro biological and in-silico strategies.** *J Biomol Struct Dyn* 2021, <https://doi.org/10.1080/07391102.2021.2018045>.
57. Wu Y, Hsieh T-C, Wu JM, Wang X, Christopher JS, Pham AH, Swaby JD-L, Lou L, Xie Z-R: **Elucidating the inhibitory effect of resveratrol and its structural analogs on selected nucleotide-related enzymes.** *Biomolecules* 2020, **10**:E1223.
58. Pettersen EF, Goddard TD, Huang CC, Meng EC, Couch GS, Croll TI, Morris JH, Ferrin TE, ChimeraX UCSF: **Structure visualization for researchers, educators, and developers.** *Protein Sci* 2021, **30**:70–82.